

Reconfigurable Graphene Annular Ring Antenna for Medical and Imaging Applications

Hamza Ben Krid*, Zied Houaneb, and Hassen Zairi

Abstract—In this article, we design a reconfigurable bandwidth based on a concentric ring slot antenna using graphene. The developed antenna has good agreement between simulated and experimental results. The use of graphene in Terahertz (THz) has shown better performance than metal, and the variation in the chemical potential of graphene provides excellent performance properties, good return loss reaching -33.288 dB, bandwidth reconfiguration from 255 GHz to 406 GHz, and a good gain. These results are promising for THz applications and particularly for the application of medical imaging. The modeling and validation are performed using the CST Simulator.

1. INTRODUCTION

In recent years, microstrip patch antennas have been very popular because of their use in various wireless applications due to their low cost, ease of manufacture, miniaturized size [1], as well as a simple patch antenna, and a simple microstrip patch antenna has a single resonance frequency [1, 2]. In this class of microstrip patch antennas, annular ring antennas are characterized by an even smaller size in the fundamental mode than the circular or rectangular patch antennas, which makes them more compact, flexible which is important for the communication and high-frequency applications [3, 4].

However, an antenna is considered to be reconfigurable when at least one of the characteristics is modifiable after its manufacture, by application of a command [5]. It must be able to adapt to its environment by modifying its operating frequency, and/or its polarization and/or operating diagram, thus offering the possibility of realizing part of the functions generally reserved for the radio stage or the treatments digital signal [5, 6]. While the concept of a reconfigurable antenna is not new, the integration of components on so-called “active” antennas going back to the 1960s, and it attracts increasing interest in this context where flexible radio approaches are developed [7–9].

As previously impossible, in 2004 at the University of Manchester (England) two physicists discovered that by isolating a layer only one atom thick, graphene is obtained from graphite as its name suggests. The latter is a simple two-dimensional sheet; it has the shape of a hexagonal pattern composed of carbon atoms [10]. Graphene is the material most studied by the scientific community for its new and unique physical properties. Indeed, it is characterized by high electric mobility greater than $2.105 \text{ cm}^2 \text{ V}^{-1} \text{ s}^{-1}$ as well as an unusual quantum Hall effect and a modulable forbidden band with good flexibility and excellent mechanical resistance, and most importantly, it is characterized by a thermal conductivity ten times higher than that of copper [11, 12].

According to its discovery, the interest for graphene has been increasing in the scientific community, thanks to its unique physical and chemical properties, and graphene is used in diverse fields like nanoelectrics, material science, photovoltaics, and engineering. In addition, graphene is already exploited in biotechnology, antibacterial materials, disease diagnosis, drug delivery, and cancer

Received 8 November 2019, Accepted 11 January 2020, Scheduled 27 January 2020

* Corresponding author: Hamza Ben Krid (Hamza.benkrid@enicar.u-carthage.tn).

The authors are with the Research Laboratory Smart Electricity & ICT, SEICT, National Engineering School of Carthage, University of Carthage, Tunis, Tunisia.

targeting [13–15]. In this article, to reconfigure and expand the bandwidth, a graphene-based concentric annular patch was placed inside a circular slot and low impedance feed line.

The increase in the thickness of the substrate allows us to have a wider bandwidth of the antenna, but this has a bad influence on the stability and radiation [16]. In terahertz, to facilitate the manufacture and improve the performance of the antenna we use the characteristic impedance of graphene to have a UWB antenna. The use of graphene improves the gain as well as avoids the skin effect of the metal and decreases the loss of the antenna [17, 18].

The paper is structured as follows. Section 2 will be devoted to the structure and dimension of the proposed structure. Section 3 deals with the conductivity of graphene. Next, Section 4 will present the comparison between metal and graphene as well as reconfiguring the bandwidth using the chemical potential of graphene. Finally, Section 5 concludes the paper.

2. DESIGN OF THE PROPOSED ANTENNA

The annular ring antenna is characterized by a miniaturized size compared to the circular patch with a wider band. In this article, in order to reconfigure the bandwidth of the antenna, a concentric annular plate is placed inside a circular slot. The relative permittivity of the TRF-43 substrate is 4.3, and a feed line is placed inside the substrate, and the substrate TRF-43 is characterized by a permittivity $\epsilon = 4.3$ and a thickness of $2 \mu\text{m}$. The concentric and circular patch is designed in graphene of thickness $0.01 \mu\text{m}$. Table 1 gives the optimized dimensional parameters of the proposed antenna.

Table 1. Parameters of the proposed antenna.

Parameters	Value (μm)
Wave length	104
Groundplan thickness	0.1
Width and length of the Substrate and groundplan	104×104
Substrate thickness	2
Graphene thickness	0.01
Width and length of the patch	92×92
R_1	10
R_2	26
Feedline length	23.59
Feedline thickness	0.30
h	2.11
L_1	24.59
L_2	16.82
W	20

3. GRAPHENE CONDUCTIVITY

The surface conductivity of graphene that is modeled as a sheet conductor is composed of two terms. One term represents the inter-band conductivity, and the other represents the intra-band term. The surface conductivity in the terahertz band can be expressed using only the first inter-band term and neglecting the second term in-band as it has no significant effect [19, 20].

The surface conductivity is as follows

$$\sigma_{\text{intra}} = -j \frac{e^2 K_B T}{\pi \hbar^2 (\omega - j2\Gamma)} \left[\frac{\mu_c}{K_B T} + 2 \ln \left(e^{-\frac{\mu_c}{K_B T}} + 1 \right) \right] \quad (1)$$

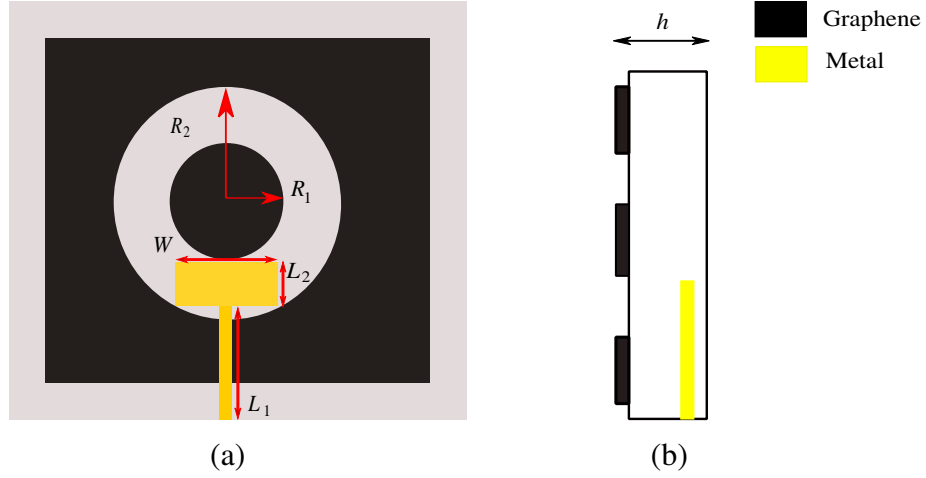


Figure 1. Proposed antenna design: (a) top view, (b) side view.

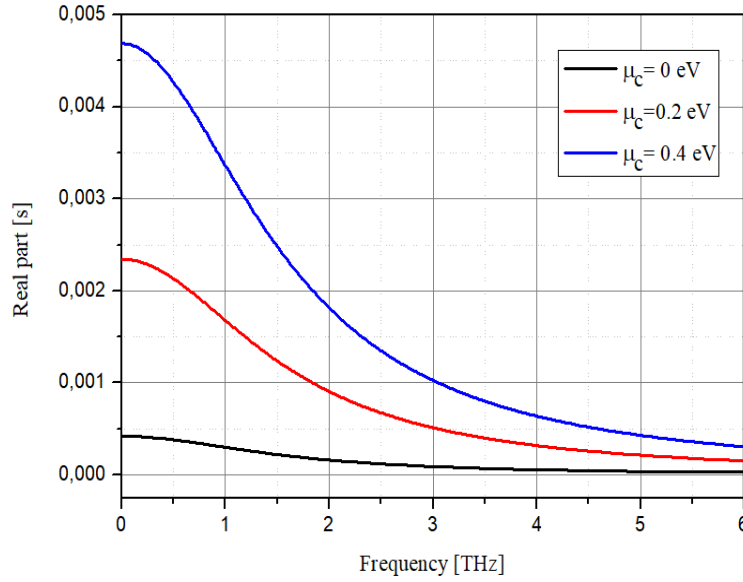


Figure 2. Real part of conductivity.

The inter-band conductivity is

$$\sigma_{\text{inter}} = -j \frac{e^2}{4\pi\hbar} \left[\frac{2|\mu_c| - (\omega - j2\Gamma)\hbar}{2|\mu_c| + (\omega - j2\Gamma)\hbar} \right] \quad (2)$$

where e is the electron charge constant, Γ the scattering rate, T the temperature, ω the angular frequency, K_B the Boltzmann, \hbar the reduced Planck's constant, and μ_c the chemical potential. Intra-band conductivity is a complex entity that can be expressed by

$$\sigma = \sigma_r + j\sigma_i \quad (3)$$

with σ_r the real part of the conductivity and σ_i the imaginary part.

Figures 2 and 3 represent the real and imaginary parts of the conductivity of graphene, respectively, as a function of frequency for different values of the chemical potential ranging from 0 eV to 0.4 eV. Here the temperature is fixed at 300 K, and the relaxation time is selected as 0.1 ps. The effect of modifying

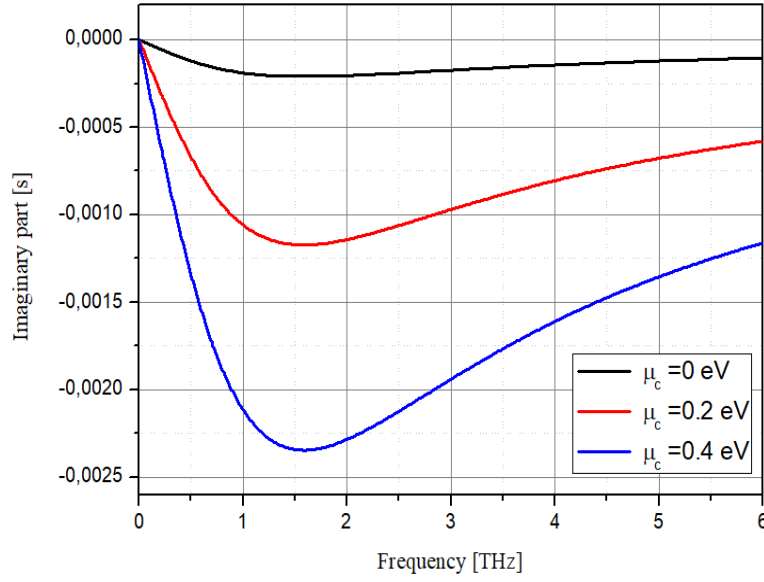


Figure 3. Imaginary part of conductivity.

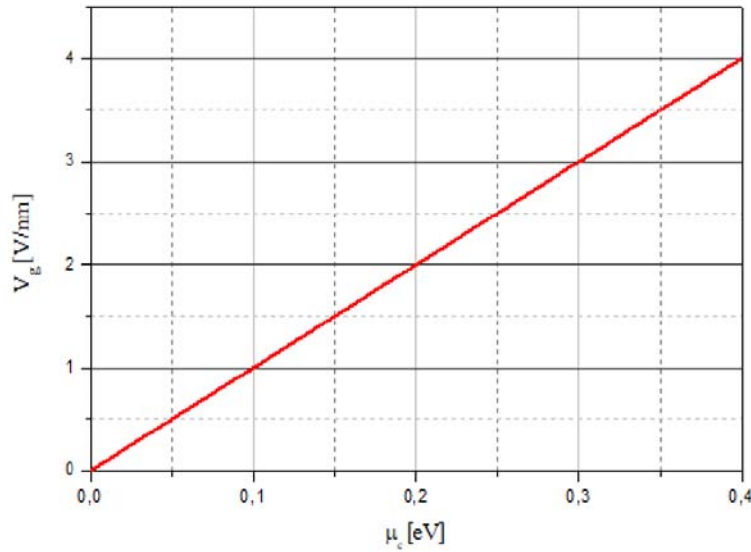


Figure 4. Voltage applied to graphene.

the chemical potential on the conductivity by the control of the polarization voltage (carrier density) can be seen from the two previous figures. The relation between the chemical potential and bias voltage is shown in Fig. 4, defined by the following equation.

$$V_g = \frac{e\mu_c^2 h}{\pi h^2 V_f^2 \varepsilon_0 \varepsilon_r} \quad (4)$$

where h is the thickness of the substrate, V_f the fermi velocity in graphene, and ε_r the permittivity of the substrate.

4. RESULTS AND DISCUSSIONS

The structure in Fig. 1 is simulated by the software CST Electromagnetic (computer simulation technology). In order to reconfigure the bandwidth of our proposed antenna, we use three values of $\mu_c = 0 \text{ eV}$, $\mu_c = 0.2 \text{ eV}$, $\mu_c = 0.4 \text{ eV}$. We use graphene with a thickness of $0.01 \mu\text{m}$ to the top layer and metal for the patch inside the substrate with a thickness of $0.2 \mu\text{m}$.

4.1. Comparative Study between Metal and No-Doped Graphene

The first simulation aims to compare the proposed antenna in the case of no-doped graphene and the same structure but replacing the graphene by the metal. Fig. 5 shows the return loss for the two simulated configurations. Fig. 5 shows that the reflection coefficients of the metal-based antenna are less adapted than that of graphene. It is quite reasonable because metal is not used in the order of THz band. On the other-hand, graphene gives better performance in terms of reflection coefficient. The return loss is reduced from -6.440 to -15.125 dB . Fig. 6 shows the distribution of the current in the antenna surface, and graphene shows better results than metal.

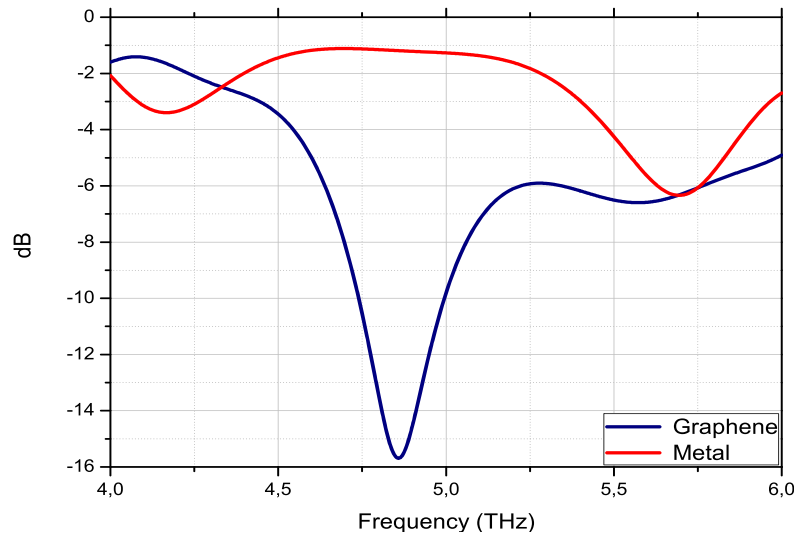


Figure 5. Comparative curves of the return loss S_{11} of no-doped graphene antenna and proposed metal antenna.

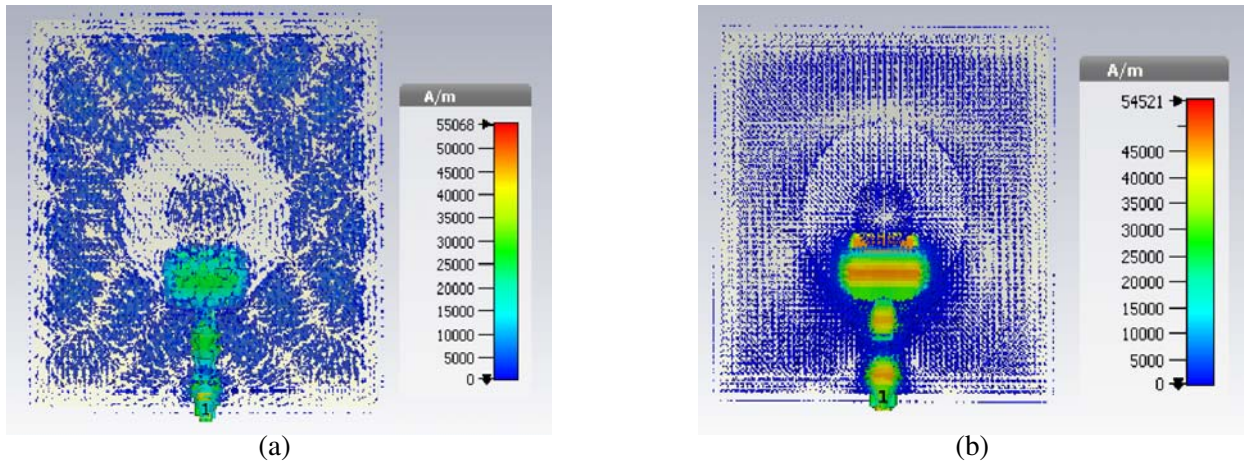


Figure 6. Current distribution surface: (a) graphene, (b) copper.

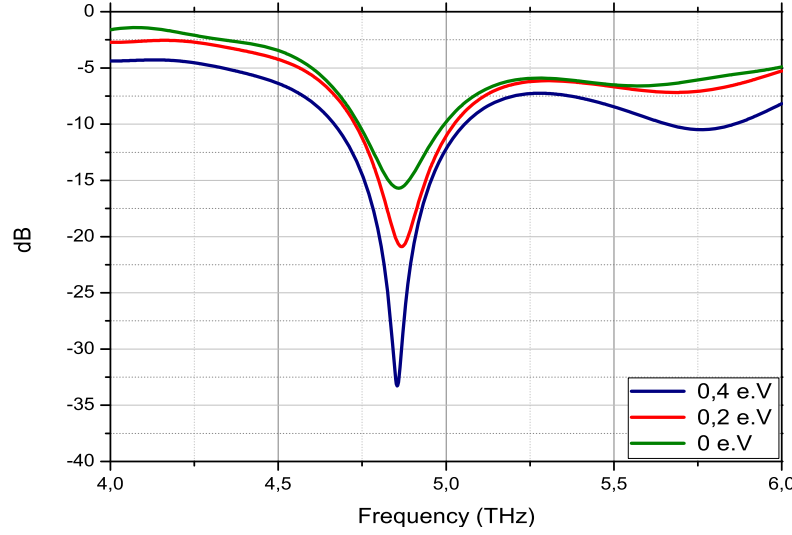


Figure 7. Return loss for the different values of the chemical potentials.

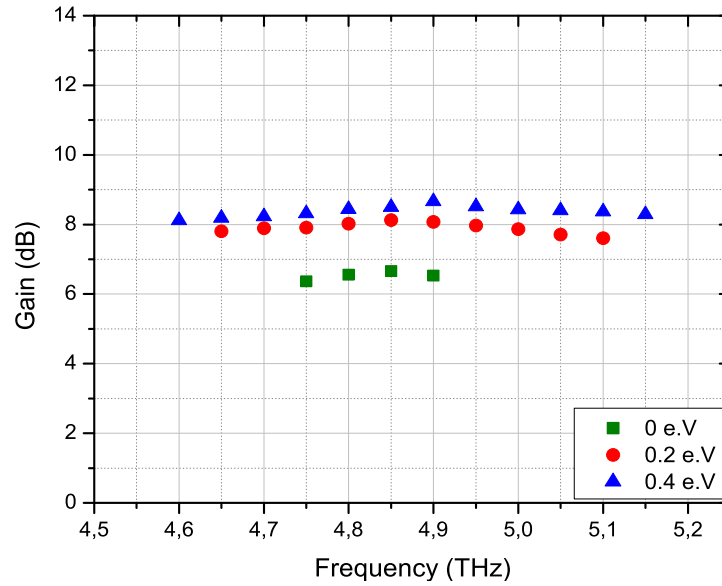


Figure 8. The simulated gain of the antenna.

4.2. Reconfigurable Antenna Proposed Using Graphene

In Fig. 7, we present results of the chemical potential reflection coefficient for different values of μ_c , which varies from 0, 0.2 to 0.4 eV. There are three resonance frequency bands for these last three values of μ_c , which cover the range of 4,667 THz to 5,055 THz. To obtain these three reconfigurations of the bandwidth, it is necessary to vary the chemical potential μ_c . For the first value of the chemical potential $\mu_c = 0$ eV, we obtain a BW = 255 GHz (4.739–4.994 THz). For the second value of the chemical potential $\mu_c = 0.2$ eV, we obtain a BW = 295 GHz (4.729–5.024 THz). The bandwidth is increased by 40 GHz, and the return loss is reduced from -15.125 to -20.896 . The last value of the chemical potential $\mu_c = 0.4$ eV. We obtain BW = 406 GHz (4.667–5.073 THz). The bandwidth is increased by 111 GHz, and the return loss is reduced from -20.896 to -33.288 .

Figure 8 shows the obtained gain values, 6.66 dB, 8.13 dB, and 8.6 dB, according to the frequency for the different values of μ_c . We observe that for $\mu_c = 0.4$ eV we obtain a better gain of 8.6 dB with

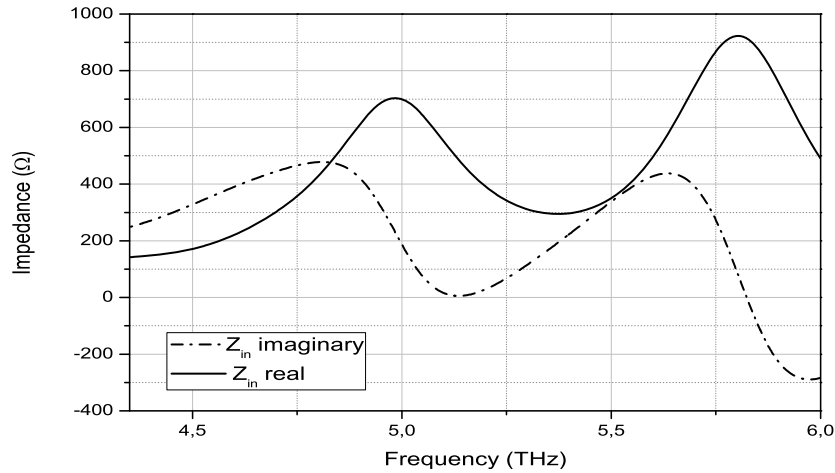


Figure 9. Real and imaginary parts of input impedance for ($\mu_c = 0$ eV).

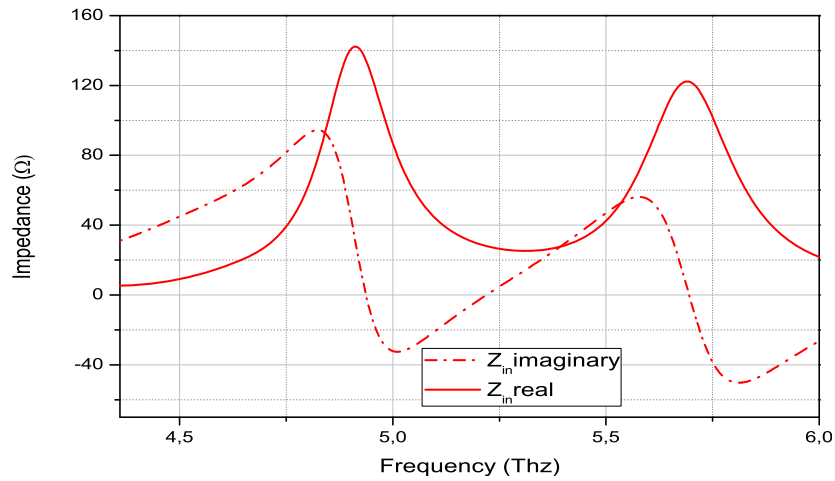


Figure 10. Real and imaginary parts of input impedance for ($\mu_c = 0.2$ eV).

Table 2. Performance of the proposed antenna for various chemical potential value.

μ_c (eV)	f_r (THz)	BW (GHz)	VSWR	Gain (dB)	Return loss (dB)
$\mu_c = 0$	4.854	255	4.860	6.66	-15.125
$\mu_c = 0.2$	4.862	294	4.866	8.13	-20.896
$\mu_c = 0.4$	4.878	406	4.852	8.6	-33.288

BW = 406 GHz.

According to Fig. 9, Fig. 10, and Fig. 11, $\mu_c = 0.4$ eV shows better adaptation.

The simulation allows us to also have the radiation patterns for the E -plane and H -plane of the antenna which are presented in Fig. 12, Fig. 13, and Fig. 14 for different values of the chemical potential, respectively. There is a variation of the antenna lobes in the E and H plans noting that the back and front lobes allow us to have a good ratio, and the radiation patterns are almost unidirectional.

The values are obtained for bandwidth (BW) and voltage standing wave ratio (VSWR) of the resonant frequency for chemical potential values from 0 to 0.4 eV. From Table 2, it can be seen that by tuning the proposed antenna, the BW increases from 255 GHz to 406 GHz, and the resonant frequency

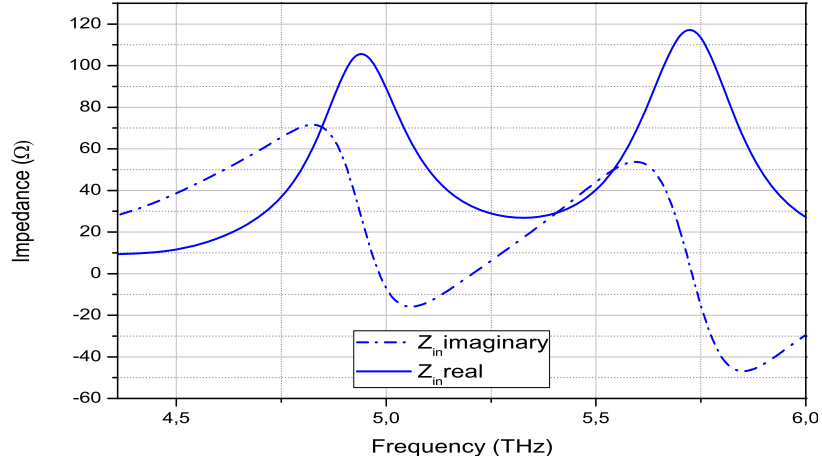


Figure 11. Real and imaginary parts of input impedance for ($\mu_c = 0.4 \text{ eV}$).

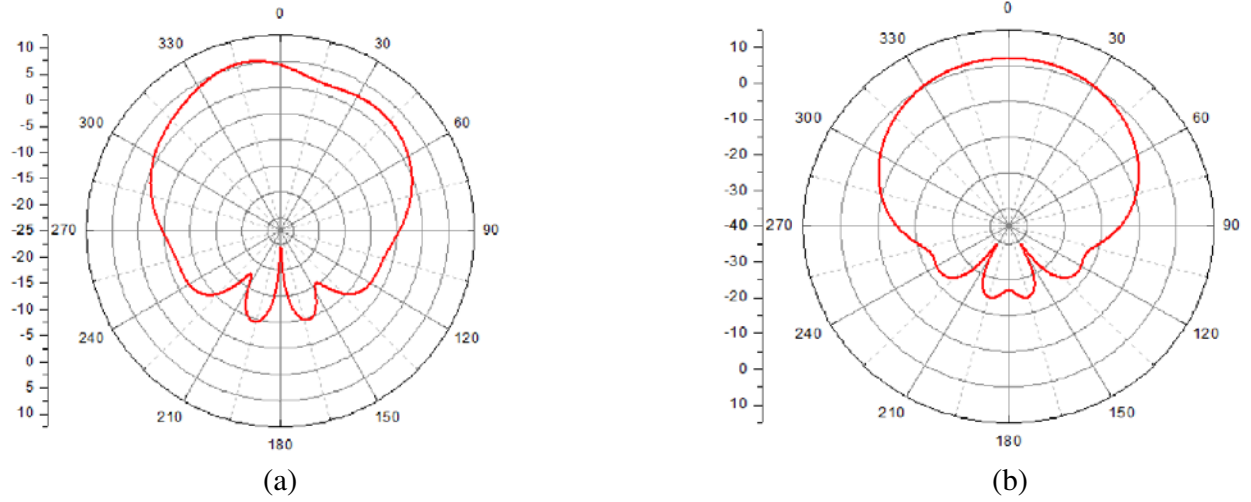


Figure 12. Radiation pattern of the proposed antenna ($\mu_c = 0 \text{ eV}$): (a) E -plane, (b) H -plane.

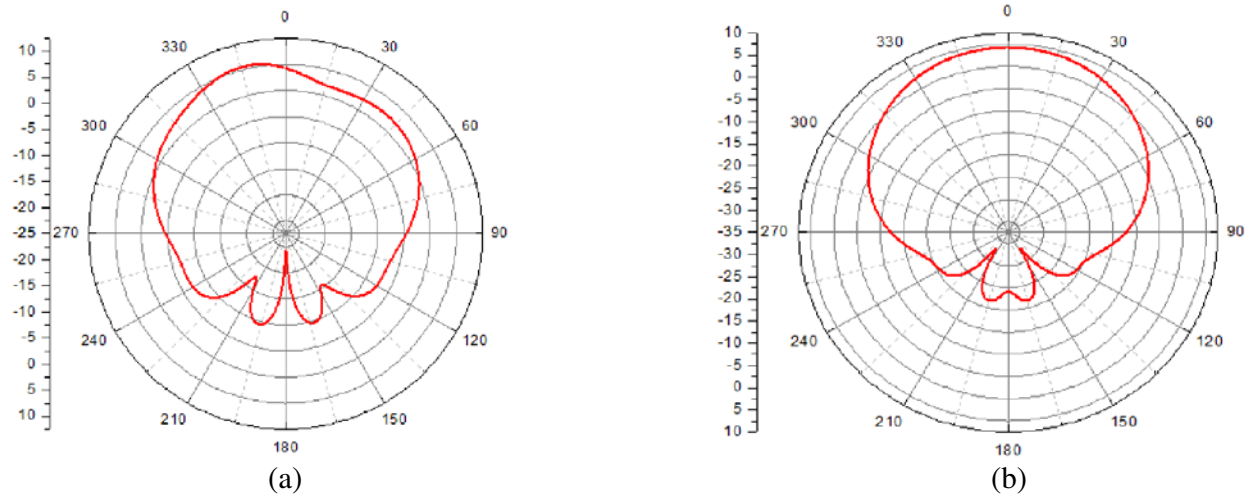


Figure 13. Current distribution surface: (a) metal, (b) graphene.

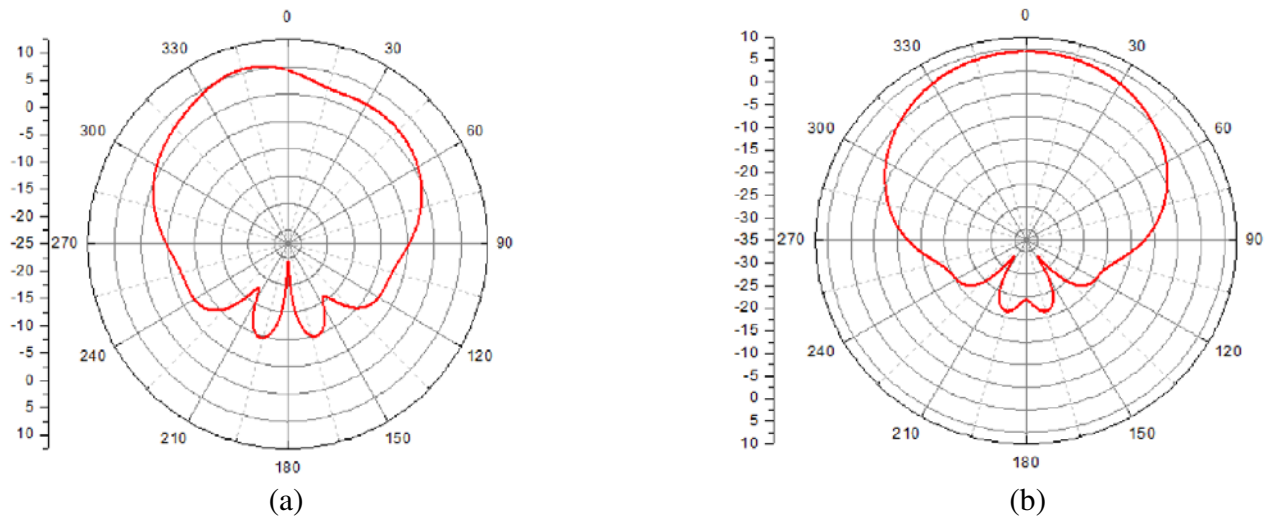


Figure 14. Radiation pattern of the proposed antenna ($\mu_c = 0.4$ eV): (a) E -plane, (b) H -plane.

varies from 4.85 GHz to 4.87 GHz. We also notice from this table that the proposed antenna has a maximum peak gain equal to 8.6 dB at the resonant frequency for the applied chemical potential value of 0.4 eV. A second valuable observation is that as the value of potential chemical increases, the antenna becomes more adaptable, and it can be seen that the best conditions are achieved with 0.4 eV for the chemical potential and with return loss reaching the maximum value of 33.28 dB.

5. CONCLUSIONS

In this paper, a graphene annular antenna intended for medical applications is proposed. The simulation is performed using the CST software while varying the chemical potential. Graphene shows better results than metal in terms of performances with a well-adapted resonant frequency. Graphene gives a tunable results in terms of bandwidth which varies between 255 GHz and 406 GHz. The variation of the chemical potential (μ_c) gives, as a result, a reconfiguration of the bandwidth with a change in the performance of the antenna.

REFERENCES

1. Gupta, N. and R. Singh, "An annular ring microstrip patch antenna for multiband applications," *International Journal of Engineering Research and Technology*, Vol. 4, 1087–1091, 2015.
2. Vasconcelos, C. F. L., S. G. da Silva, M. R. M. L. Albuquerque, J. de Ribamar Silva Oliveira, and A. G. d'Assunção, "Annular ring microstrip patch antenna on a double dielectric anisotropic substrate," *PIERS 2009 in Moscow Proceedings*, 18–21, Moscow, Russia, August 18–21, 2009.
3. Kaur, H. and M. Aggawal, "Design of microstrip patch antenna by introducing defected ground structure," *International Journal of Advanced Computer Science and Application*, Vol. 99, 14–24, 2018.
4. Saturday, J., M. Udofia, et al., "Design of dual band microstrip antenna using reactive loading technique," *Mathematical and Software Engineering*, Vol. 2, 114–121, 2016.
5. Costantine, J., et al., "Reconfigurable antenna design and application," *Proceeding of the IEEE*, Vol. 103, 424–437, 2015.
6. Azizi, M. K., M. A. Ksiksi, H. Ajlani, and A. Gharsallah, "Terahertz graphene-based reconfigurable patch antenna," *Progress In Electromagnetics Research Letters*, Vol. 71, 69–76, 2017.
7. Mazlouman, S., M. Soleimani, et al., "Pattern reconfigurable square ring patch antenna actuated by hemispherical dielectric elastomer," *Electronics Letters*, Vol. 47, 164–165, 2011.

8. Surface, H., Y. Huang, et al., "Design of a beam reconfigurable THz antenna with graphene-based switchable," *IEEE Transactions on Nanotechnology*, Vol. 11, 836–842, 2012.
9. Christos, G., et al., "Reconfigurable antenna for wireless and space application," *Proceeding IEEE*, Vol. 100, 2250–2261, 2012.
10. Georgakilas, V., *Functionalisation of Graphene*, 21–23, Wiley-VCH, 2014.
11. Kuman, K., et al., *Graphene-based Polymer*, 8–11, Springer, 2015.
12. Choi, W. and J. Lee, "Graphene synthesis and application," *Nanomaterials and Their Application*, 10–13, 2012.
13. Liang, T., Y. Kong, et al., "From solid carbon sources to graphene," *Chinese Journal of Chemistry*, Vol. 34, 32–40, 2015.
14. Jang, S., E. Hwang, et al., "Graphene-graphene oxide floating gate transistor memory," *Small Nano Micro*, Vol. 11, 311–318, 2015.
15. Dong, Y. and P. Liu, "Dual-band reconfigurable terahertz patch antenna with graphene-stack-based backing cavity," *IEEE Antennas and Propagation Society*, Vol. 15, 1541–1544, 2016.
16. Zhang, H. and Y. Jiang, "A broadband terahertz antenna using graphene," *11th International Symposium on Antennas, Propagation and EM Theory (ISDPE)*, 149–152, 2016.
17. Inum, R., M. Rana, et al., "Performance analysis of graphene based nanodipole antenna on staked substrate," *2nd International Conference on Electrical Computer and Telecommunication Engineering (ICECTE)*, 1–4, 2016.
18. Bala, R., A. Marwaha, et al., "Investigation of graphene based miniaturized terahertz antenna for novel substrate materials," *Engineering Science and Technology, an International Journal*, 531–537, 2015.
19. Hlali, A., Z. Houaneb, and H. Zairi, "Dual-band reconfigurable graphene-based patch antenna in terahertz band: Design, analysis and modeling using WCIP method," *Progress In Electromagnetics Research C*, Vol. 87, 213–226, 2018.
20. Hlali, A., Z. Houaneb, et al., "Tunable filter based on hybrid metal-graphene structures over an ultrawide terahertz band using an improved wave concept iterative process method," *Optik*, Vol. 181, 223–231, 2019.